

ZAHA: Introducing the Level of Facade Generalization and the Large-Scale Point Cloud Facade Semantic Segmentation Benchmark Dataset

Olaf Wysocki¹, Yue Tan¹, Thomas Froech¹, Yan Xia^{1,3}, Magdalena Wysocki^{1,3},
Ludwig Hoegner², Daniel Cremers^{1,3}, Christoph Holst¹

¹ Technical University of Munich, ² Munich University of Applied Sciences,
³ Munich Center for Machine Learning (MCML)

(olaf.wysocki, yue.tan, thomas.froech, yan.xia, magdalena.wysocki,
ludwig.hoegner, cremers, christoph.holst)@tum.de

Abstract

Facade semantic segmentation is a long-standing challenge in photogrammetry and computer vision. Although the last decades have witnessed the influx of facade segmentation methods, there is a lack of comprehensive facade classes and data covering the architectural variability. In ZAHA¹, we introduce Level of Facade Generalization (LoFG), novel hierarchical facade classes designed based on international urban modeling standards, ensuring compatibility with real-world challenging classes and uniform methods' comparison. Realizing the LoFG, we present to date the largest semantic 3D facade segmentation dataset, providing 601 million annotated points at five and 15 classes of LoFG2 and LoFG3, respectively. Moreover, we analyze the performance of baseline semantic segmentation methods on our introduced LoFG classes and data, complementing it with a discussion on the unresolved challenges for facade segmentation. We firmly believe that ZAHA shall facilitate further development of 3D facade semantic segmentation methods, enabling robust segmentation indispensable in creating urban digital twins.

1. Introduction

Facade semantic segmentation is a fundamental issue in photogrammetry and computer vision [51]. The issue has become compounded thanks to such innovative architects as Zaha Hadid, challenging the standard assumptions of the wall's planarity, utilizing new materials, and mingling old with new architecture.

Throughout the years, various methods have been created for image-based facade segmentation, predominantly

facilitated by datasets of annotated facade images [26, 32, 38]. Although the segmentation performance on the ortho-rectified images can reach even 90% [32], the 2D-image nature hinders the immediate understanding of 3D scenes, limiting the 3D facade segmentation capabilities. The striking example are intruded and extruded facade elements, which have been under-explored, owing to inability to capture their structure and depth with 2D ortho-rectified images. These flaws impact other research fields frequently relying on a 3D facade semantic segmentation, such as 3D semantic building reconstruction at a high level of detail [66], finding its applications in simulating flood risk [1] or testing automated driving functions [45], among others [61, 64].

Recent developments have demonstrated that mobile laser scanning (MLS) devices can fill this 3D data gap: Once they are mounted on a mobile platform, they deliver dense, street-level point clouds, enabling capturing a 3D urban environment and, thus, 3D facade geometry (Fig. 1) [68]. This trait has sparked significant growth in urban point cloud benchmark datasets [23, 63] and the development of many semantic segmentation methods [30, 52, 68].

Yet, one of the crucial impediments in developing facade segmentation methods is the facade classes heterogeneity; leading to misinterpretations of facade element characteristics and hampering the development of a large-scale, high-variability data. This overlooked issue also impedes applying semantically segmented facades directly to the 3D semantic building reconstruction tasks since they mismatch taxonomically and geometrically the well-established modeling classes defined in the international standards [17, 66, 68]. Another key issue pertains to the limited annotated facade samples for methods' training and validation. Only two relatively small datasets comprise facade-level classes: TUM-FAÇADE [63] and ArCH [35], which however either focus on a single university dataset or on only specific cul-

¹Project page: <https://github.com/OloOcki/zaaha>

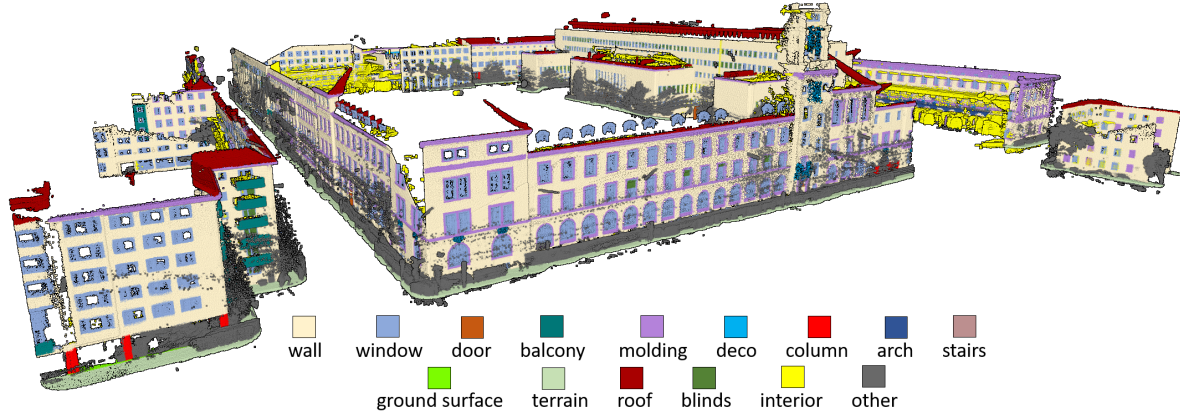


Figure 1. ZAHA: The dataset comprising 66 facades of various architectural style yielding over 601 million facade-level annotated terrestrial point clouds with distinct 15 facade-relevant classes.

tural heritage buildings, respectively.

To tackle the challenges mentioned above, in this paper, we present the following contributions:

- Proposing Level of Facade Generalization (LoFG): Novel hierarchical facade classes designed based on international facade-related standards;
- Realizing LoFG concept on the introduced, to date, the largest point cloud facade semantic segmentation dataset, boasting 601 million points (Fig. 1);
- Identifying outstanding challenges of the 3D facade semantic segmentation based on the extensive experimental and research analysis.

2. Related Works

2.1. Facade-Related Point Cloud Datasets

For many years researchers have invested a great deal of effort in introducing multiple image-based facade segmentation datasets for methods development [12, 26, 43, 51, 56]. For instance, in one of the first works over a decade ago, the eTRIMS dataset has introduced 60 facade images [26] and eight facade-relevant labels. Yet, these and following works [56] have been inconsistent with their facade elements definitions and have been limited concerning intruded and extruded 3D facade elements (e.g., arches).

Unlike the image-based data, the point cloud datasets for facade segmentation remain in their infancy (see Table 1). Although many benchmarks are devoted to 3D urban semantic segmentation, only ArCH [35] and TUM-FAÇADE [63] datasets comprise facade-level classes. Yet, the ArCH dataset focuses on cultural heritage buildings, which trait renders it infeasible for methods' testing on common facade types; Whereas the TUM-FAÇADE represents solely university buildings, and its relatively small size of 14 facades

makes it insufficient for extensive methods' development; Furthermore, such important facade classes as *balcony* have no data representation.

Interestingly, the Oakland 3D [37] and the Paris-rue-Madame [47] datasets also cover some aspects of the facade element classes. Oakland 3D comprises only a few facade-related classes, inadequately capturing the key facade elements (e.g., windows are absent). Similarly, the Paris-rue-Madame dataset is restricted to merely wall lights, wall signs, and balcony plants, limiting its application for facade segmentation. Another limitation of the datasets comprising facade classes is their limited size: TUM-FAÇADE and ArCH comprise around 100 million points, Paris-rue-Madame scores 20 million, and Oakland 3D has less than 2 million annotated points.

Moreover, as shown in Table 1, the class variability among the datasets is high, which hinders the standardized comparison between benchmarks and their reported segmentation results. This trend is underscored by their high class-wise standard deviation of approximately 13, ranging from eight to up to 50 classes (excluding the non-labeled datasets). On the other hand, multiple international organizations exist that create standardized descriptions of urban objects, including facade elements. One of the leading bodies is Open Geospatial Consortium (OGC), which has been releasing the international CityGML standard [17, 25], providing a comprehensive description of geometries, structures, taxonomies, and aggregations at the scale of buildings but also entire countries [24]. Its wide adoption is highlighted by the example of more than 200 million open-data 3D building models available in Switzerland, Germany, the United States, the Netherlands, and Poland, among others [65]. The complementing sources for facade description are the Art and Architecture Thesaurus (AAT) and the Industry Foundation Classes (IFC) standard, which are widely applied in the architecture and civil engineering domains

Table 1. Point cloud benchmark datasets for testing urban semantic segmentation.

Name	Year	Sensor	World	# Classes	Facade-level classes?	# Facade-labeled points	Various facade types?	Hierarchical classes?
Oakland 3D [37]	2009	MLS	real	44	~	~1.6 M	✗	✗
ETH PRS [29]	2012	TLS	real	0	✗	✗	-	✗
Sydney Urban Objects Dataset [8]	2013	MLS	real	26	✗	✗	-	✗
Paris-rue-Madame database [47]	2014	MLS	real	27	~	~20 M	✗	✗
iQumulus [57]	2015	MLS	real	8	✗	✗	-	✗
TUM-MLS-2016 [72]	2016	MLS	real	9	✗	✗	-	✗
semantic3D.net [18]	2017	TLS	real	9	✗	✗	-	✗
Paris-Lille-3D [44]	2018	MLS	real	50	✗	✗	-	~
SynthCity [15]	2019	MLS	synthetic	9	✗	✗	-	✗
A2D2 [13]	2020	MLS	real	38	✗	✗	-	✗
ArCH [34]	2020	TLS/MLS/UAV	real	10	✓	136 M	✗	✗
Toronto-3D [52]	2020	MLS	real	8	✗	✗	-	✗
Whu-TLS [10]	2020	TLS	real	0	✗	✗	-	✗
BIMAGE Datasets [4]	2021	MLS	real	0	✗	✗	-	✗
KITTI-360 [31]	2021	MLS	real	19	✗	✗	-	✗
Paris-CARLA-3D [9]	2021	MLS	real/synthetic	23	✗	✗	-	✗
TUM-FAÇADE [63]	2022	MLS	real	17	✓	118 M	✗	✗
HelixNet [33]	2022	MLS	real	9	✗	✗	-	✗
SUD [14]	2023	MLS	real	8	✗	✗	-	✗
ZAHA (ours)	2024	MLS	real	15	✓	601 M	✓	✓

[28, 35], for instance, in the building information modeling (BIM) context [24].

The hierarchical understanding of the facade description has been also overlooked by all of the investigated datasets. Yet, in the context of building modeling standards three level of details (LoDs) are recognized [27], acknowledging varying data availability, methods’ performance on limited data, and the downstream task requirements. Only Paris-Lille-3D [44] follows the similar concept for point cloud segmentation, where they provide hierarchization of urban scenes. However, the classes do not describe facade elements, are not based on international standards, and many classes have none or limited data representation in the introduced data realization.

2.2. 3D Facade Semantic Segmentation Methods

The advent of the aforementioned image-based benchmarks has sparked advancements in facade segmentation using images. Various methods have been proposed to tackle this challenge, starting with non-learning [38, 51], grammar-based [6, 36], and recently deep learning approaches [19, 22, 32]. However, 2D-image-reliance restricts the methods to 2D image information, which hampers its direct application to the 3D facade segmentation and thus limits capturing the facade intruded and extruded elements depth [19, 66].

A different strategy focuses on direct 3D facade segmentation using laser scanning point clouds, leveraging the detailed and accurate depth information provided by MLS point clouds [67, 68]. Recently, the deep learning approaches have shown great potential in 3D point cloud segmentation [41, 42, 71]. Qi et al., [41] present the PointNet

architecture, which enables efficient point-wise 3D point cloud segmentation on unordered sets. Following works [42, 60, 71], have further improved segmentation performance.

Notably, significant advancements in point-wise, learning-based techniques have been applied to 3D facades segmentation as well [3, 16, 34, 53, 62]. They typically perform well on the planar-like, ubiquitous classes, reaching around 75% in F1 score for the wall class when applying DGCNN [40]. However, the research shows the off-the-shelf methods face challenges when dealing with sparse- and under-represented classes, such as decorations, moldings, stairs, windows, and doors [34, 40]. Essentially, facing the typical long-tail data distribution recognition problem of real-world data [7, 11, 69, 70]. This issue is reflected in, for example, low scores for the standard Point Transformer network [71], which can merely reach F1 scores of 49%, 2%, and 48%, for window, door, and molding class, respectively [62]. Also, as reported by Pierdicca et al., recall scores for column, arc, decoration, door, and stair classes can oscillate around 0-1% for PointNet and PointNet++ [40].

Yet, caution must be exercised while analyzing the reports, as the tests are currently inadequate, performed on heterogeneous classes and small datasets comprising a limited number of facades and their types [34, 63]; under-scoring the need for developing classes harmonization and large-scale point cloud facade datasets. The methods’ performance is also dependent on the granularity of the target classes, where the reception field and sampling strategies play pivotal role [54]. This characteristic results in varying performance for dense-distribution objects (e.g., walls)

and sparse and thin objects (e.g., windows) depending on network assumptions. As such, the evaluation at various generalization facade levels is of pivotal importance.

3. The LoFG and Its Realization

3.1. 3D Semantic Facade Classes

As shown in Table 1, there is a lack of high facade variability and hierarchical facade-level point cloud benchmarks available. Understanding the need for 3D facade semantic segmentation gradation due to different methods' assumptions, downstream tasks, and data availability, we introduce LoFG, where we distinguish three levels of facade generalization: LoFG1, LoFG2, and LoFG3. This concept and its presented logic in Fig. 3 aim to allow for precisely formulating 3D facade semantic segmentation and classification problems. Furthermore, it shall enable seamless adoption of such techniques as transfer learning [48], epoch-to-epoch labels transferring [46], and a unified comparison of different methods.

Within the scope of this work, we introduce the harmonized 15 facade classes (LoFG3) generalizing to five classes (LoFG2), and one abstract class (LoFG1), developed concerning the international urban modeling standards such as CityGML, IFC, and Art and Architecture Thesaurus (AAT), and related works [34, 63]. The detailed description of the introduced classes is provided in Tab. 2 whereas the visualization is in Fig. 1 and Fig. 2. Moreover, owing to leveraging the modeling standards the presented classes correspond to the established 3D semantic reconstruction classes, aiming to provide a seamless platform for applying the 3D facade semantic segmentation results to the 3D facade semantic reconstruction [17, 27, 66].

The LoFG3 describes the most detailed facade representation comprising 15 facade classes of *ground surface*, *terrain*, *molding*, *deco*, *wall*, *stairs*, *balcony*, *column*, *arch*, *blinds*, *door*, *window*, *roof*, *interior*, and *other* (for the detailed description see Tab. 2). The LoFG2 aggregates the 15 classes of LoFG3 into five less detailed classes based on syntactic, semantic, and geometrical analysis, as we illustrate in Fig. 3. The group *facade & its vicinity* represents the abstract class and is referred to as LoFG1.

Note that the LoFG is driven mainly by the semantics of facade elements and their structural definition and not sole geometrical representation. For example, *roof* is often regarded as a structural element of a building; however, in the case of terrestrial-acquired datasets, roofs are barely within the scanner field-of-view and thus resemble noise, for example, shown in [63] or in Fig. 1, Fig. 2. Furthermore, the ground and terrain classes are also clearly defined in the international standards and are considered key parts of a facade, e.g., the intersection of *terrain* with a facade is essential in establishing the total facade height, while *ground*

surface is vital in analyzing overarching structures and their volumetric extent, e.g., underpasses. Another example are the classes *windows* and *blinds*, which at LoFG3 are separate, owing to their different features, functions, and importance of such separation for window segmentation [55, 66]; Yet, at LoFG2 they are aggregated, as a blind is indissolubly linked to a window.

3.2. Data Acquisition

Based on the conducted research (Tab. 1) and seeing the potential of already created urban-related point cloud benchmarks, we present an approach to reducing the workload while developing new benchmark datasets. This reduction is achieved by enriching existing benchmarks with facade-related semantics. The data acquired for the ZAHA dataset stems from the open dataset of TUM-MLS-2016 [72], featuring a challenging, urban environment with real-world, dense, and georeferenced MLS point clouds. The measuring campaign is performed within the city of Munich, Germany. We utilize this dataset owing to its versatile architectural style of buildings built between the late 19th and early 21st century and different facade functions ranging from regular dwellings, educational, cultural heritage, shops, and traffic underpasses. Notably, the datasets are subject to active development, including level of detail (LoD)3 building models, which may be used as an additional validation set [2].

3.2.1 Mobile Laser Scans

The used TUM-MLS-2016 relies on the Mobile Distributed Situation Awareness (MODISSA) platform, employing two Velodyne HDL-64E LiDAR sensors obliquely mounted at the front and two Velodyne VLP-16 sensors at the rear of the van-type vehicle. The inertial navigation system is complemented by real-time kinematic (RTK) correction data from the German satellite positioning service (SAPOS), enhancing accurate georeferencing throughout the data collection process [5, 72]. Due to large float numbers, we present the data in a local coordinate reference system (CRS) and attach the transformation matrix, which enables back-transformation of the projected CRS of UTM 32 (EPSG: 25832).

3.2.2 Semantic Annotation

We leverage the georeferencing to support the annotation and data extraction process. We acquire cm-grade footprints from governmental, open-data CityGML LoD2 building models [58], which are available in the same CRS as the obtained point clouds. To extract the facades and their vicinity, we draw a buffer around each building footprint with a radius of 3m. Furthermore, in this process, each



Figure 2. Selected facades of ZAHA. The dataset comprises 15 classes distributed over a diverse facade styles and functions, presenting a versatile training and testing segmentation scenario.

Table 2. Our proposed classes (*Class*) for the ZAHA point cloud benchmark dataset. We aim to unify testing of 3D facade segmentation methods and directly link to the existing semantic 3D building modeling standards, such as CityGML [17].

Index	Class	Description	Corresponding building standard class [17]	Corresponding building standard function [49,50]
1	wall	Excluding any decorative elements	WallSurface	-
2	window	Including on-surface reflections; excluding any decorative elements	Window	-
3	door	Including garage doors and gates	Door	-
4	balcony	Excluding columns and alike supportive structures	BuildingInstallation	1000, Balcony
5	molding	Decorative elements mainly adjacent to a facade (e.g., cornices)	BuildingInstallation	1070, Other
6	deco	Decorative elements mounted to a facade (e.g., flags, gargoyles, lights)	BuildingInstallation	1070, Other
7	column	Excluding cornices (cornice → molding class)	BuildingInstallation	1011, Column
8	arch	Including only surfaces oriented downwards (including outer ceilings)	BuildingInstallation	1008, Arcade
9	stairs	Excluding column alike supportive structures	BuildingInstallation	1013, Stairs
10	ground surface	Any ground points inside a building envelope (e.g., thoroughfare)	GroundSurface	-
11	terrain	Any ground points outside a building envelope (e.g., sidewalks)	-	-
12	roof	Any surfaces representing a roof structure (incl. dormers)	RoofSurface	-
13	blinds	Window closures open or closed	BuildingInstallation	1070, Other
14	interior	Measurements that reflect within a building envelope, excluding ground points	-	-
15	other	Any other elements, noise	-	-

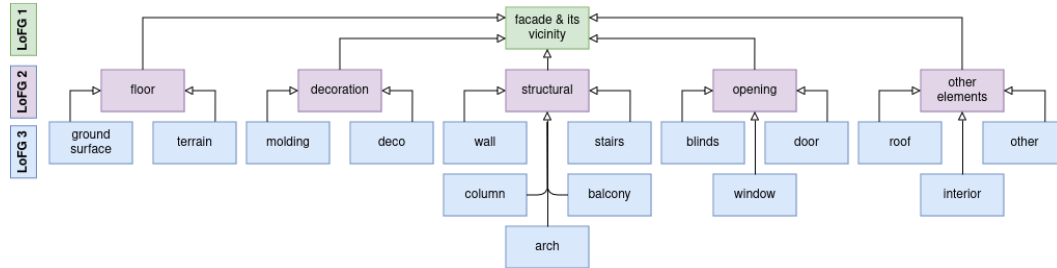


Figure 3. Level of Facade Generalization (LoFG): Primary 15 classes (blue) representing LoFG 3 at the finest level of generalization. These aggregate into coarser LoFG 2 (purple) based on their geometrical and semantical representation; The LoFG 1 (green) is designed as an abstract class allowing to group elements describing facade. Such hierarchical and harmonized representation offers adaptability to the downstream tasks of the built environment, addresses imbalanced facade datasets (long-tail), and allows for various but unified methods’ testing.

point cloud obtains its corresponding unique global identification (ID) of the building entity, matching the governmental database and thus enabling model-to-point-cloud comparison.

The manual annotation of point cloud entities is performed using Semantic Segmentation Editor [21]. The point clouds are divided into batches of approximately four million points, considering software and hardware capabilities and the operator’s ability to discern various facade features. We expand the software annotation set to accommodate our specific classes, outlined in Tab. 2, and create the setup file available in our repository. After the point clouds are merged back into entities, another round of manual inspection is applied to minimize the manually induced errors between batches. Here, we employ another software, Cyclone 3DR [20], to reduce errors induced by differences in visualization and annotation tools. For the first round of annotations, we estimate that depending on the complexity of an object, labeling requires between seven to 23 hours per building, averaging approximately six hours per facade. The following correction round of annotations requires approximately two hours per facade.

3.3. Main Benchmark Challenges

We believe that the main challenges while developing the methods performing using the ZAHA classes and dataset are as follows:

- **Classes relevant to the built environment** We introduce LoFG that harmonizes the so-far unstructured facade element classes, whereby we utilize the facade-related international standards. This characteristic ensures a homogeneous comparison of the developed algorithms and exposes the dataset to the practical challenges of the built environment. Furthermore, different levels of generalization allow the testing of various methods’ assumptions. Such design also challenges the current methods, as such classes are often highly imbalanced, see the common long-tail recognition issue in [7, 69, 70] and in our Fig. 4.
- **Facade type variations** Unlike the other facade-related datasets, we present 66 facades in various architectural styles and function types, having more than four times as many points for training and validation when compared to the largest datasets to date [35, 63]. This trait allows testing the generalization capabilities of 3D facade semantic segmentation algorithms. Simultaneously, it poses a scientific challenge in designing a generic method agnostic to the architectural facade types.
- **Consumer-grade MLS measurements** We provide the non-filtered point cloud acquired with an off-the-shelf LiDAR devices (Velodyne). No special noise

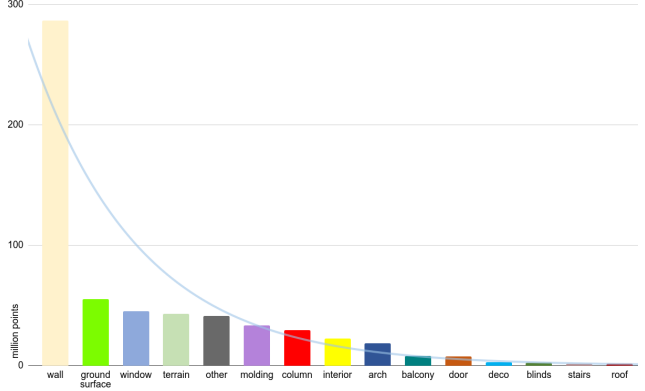


Figure 4. Head and long-tail (blue line) point-per-class distribution in ZAHA: The typical challenge of the real-world recognition tasks.

corrections and dynamic object removal are applied; interior reflections and adjacent to facade objects are kept, too. Furthermore, the given point cloud comprises only geometrical representation and no spectral information. As such, the dataset yields a challenging, real-world, and raw point clouds, useful for testing not only facade but also any generic semantic segmentation method.

4. Experiments

We conducted the experiments on the ZAHA benchmark dataset comprising 601 million semantic-annotated points². The validation set comprised typical residential facades, educational and cultural heritage facades, and facades with an underpass. The test set reflected in functions the validation set. We designated the rest of the facades for training. In our training setup, we also ensured that training, validation, and test data subsets each covered all 15 (LoFG3) and five (LoFG2) introduced classes; Consequently, the applied training and testing methods were exposed to each facade class. We also evaluated the introduced LoFG classes by applying the same training routine to both LoFG2 and LoFG3 levels and comparing the results.

4.1. Baseline Semantic Segmentation Methods

To investigate the unresolved 3D facade segmentation challenges, we tested a set of well-established semantic segmentation networks and metrics along with their original implementations on ZAHA (see the supplement for more settings’ details). To evaluate the networks’ performance, we used Overall Accuracy, Precision, Recall, and Jaccard Index, also known as Intersection over Union (IoU) [30, 40, 62]. Our methods selection was not only dictated by their performance reported in other urban-related works

²Project page: <https://github.com/OloOcki/zaha>

and datasets [16, 34, 40, 52, 59] but also by their feature extraction principles:

- **PointNet** presented by Qi et al., [41] is a seminal work in a direct point cloud understanding. The method is permutation invariant, learns point-wise local features, and allows for understanding the global scenes.
- **PointNet++** [42] improves its PoinNet predecessor by hierarchical understanding. Thus enabling more effective capture of local structures, especially in the context of fine-grained object segmentation.
- **Point Transformer (PT)** [71] utilizes the language-understanding-inspired self-attention mechanism, weighing the importance of different elements in a sequence when processing each element. It also has positional encoding, as the transformers do not capture the point position but rather sequences.
- **DGCNN** [60] leverages graph structures for learning the point set semantics, as it constructs dynamic edge convolutional graphs based on the input point clouds. It uses the k-nearest neighbors graph to capture local structures and a farthest point sampling strategy to aggregate global context.

5. Results and Discussion

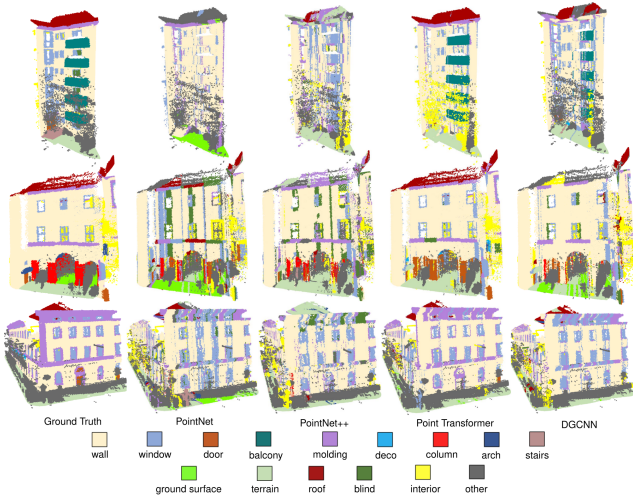


Figure 5. LoFG3 inference on the test set comprising residential (top), underpass and cultural heritage (middle), and university buildings (bottom).

5.1. Well-Performing Class Segmentation

Our experiments corroborate the research consensus that classes that are well-represented and characterized by planar geometries are likely to be correctly segmented. As we

Table 3. LoFG3 test: OA, μ P, μ R, μ F1, μ IoU, and F1 scores per class (in percentages, top scores bold).

Method	PointNet	PointNet++	Point Transformer	DGCNN
OA	59.9	66.4	75.0	71.1
μ P	46.1	37.8	52.7	53.6
μ R	42.2	35.9	54.7	45.8
μ F1	38.7	34.8	52.1	44.5
μ IoU	26.4	25.6	41.6	33.4
wall	61.1	68.5	76.8	83.8
window	25.6	26.3	43.1	64.1
door	13.5	7.8	19.8	21.6
balcony	25.1	0.0	77.5	66.7
molding	22.5	43.4	58.0	57.5
deco	0.0	0.0	5.0	0.0
column	22.4	33.4	0.0	37.2
arch	19.2	25.4	50.2	2.6
stairs	16.0	0.0	7.5	5.6
ground surface	12.0	0.0	24.4	21.3
terrain	53.5	53.5	57.6	68.0
roof	18.7	6.8	66.3	57.4
blinds	4.6	2.3	18.5	20.0
interior	59.7	69.1	72.8	88.0
other	42.7	47.1	70.6	74.1

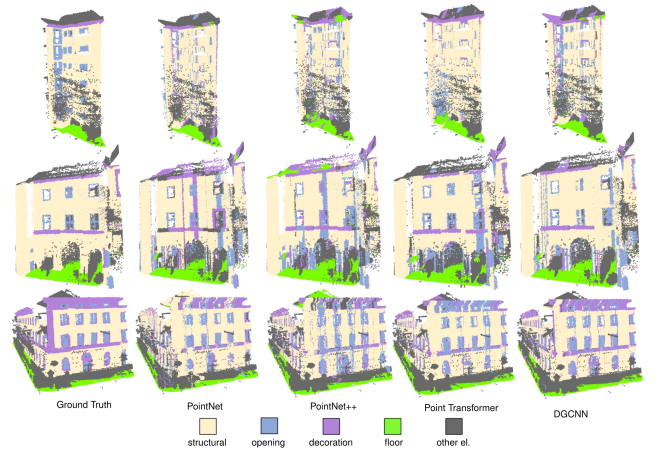


Figure 6. LoFG2 inference on the test set comprising residential (top), underpass and cultural heritage (middle), and university buildings (bottom); color-coding according to the most prominent merged sub-class.

show in Figure 5 and Figure 6, this trend is reflected in both generalization levels LoFG2 and LoFG3. The most prominent example for the LoFG3 is the *wall* class, which was the overall best-performing class with a median score of 73% (Tab. 3) across all the applied networks. For the LoFG2, it was the *floor* class comprising primarily planar-like objects that achieved a high median F1 score, reaching approximately 91% across the tested baseline methods (Tab. 4). Interestingly, also *interior* and *other* classes were reliably distinguished with up to 88% and 74% F1 scores, respectively (Tab. 3). They differentiate themselves strongly by exposing highly unstructured local patterns followed by structured global patterns, i.e., outside-inside of a facade.

5.2. Challenging Class Segmentation

Confirming our hypothesis, one of the most challenging classes was *deco*, scoring at best approximately 5% (Tab. 3) and remained largely unsegmented, as shown in Fig. 5. We attribute it to the high structure complexity, uniqueness among the samples, and high under-representation, i.e., being at the long tail of sample distribution (see Fig. 4 for the distribution). When aggregated in LoFG2 with *molding*, the score increased and reached, on average, 48%; as such, however, remaining an unresolved challenge.

As shown in Fig. 5 and Fig. 6, the *window* and *door* classes, which are the most prominent facade features, yet typically label-sparse due to their translucent main parts, were merely partially segmented. As our experiments in Tab. 3 show, *window* at best scored 64%, while *door* merely 22%; Also, the related *blinds* class scored at best 20%. When generalized to LoFG2 as *opening*, their performance reached at best 66%. Oscillating in the range of scores of 50% and less were also *arch*, *stairs*, *ground surface*, *column*, *molding*, and *roof*; underlining the need for designing more robust 3D facade segmentation methods.

5.3. Level of Facade Generalization (LoFG)

Our experiments show the usability of the proposed aggregation hierarchy design as a concept addressing 3D semantic facade segmentation at different generalization levels while maintaining facade-related semantics. As ex-

Table 4. LoFG2 test: OA, μP , μR , $\mu F1$, μIoU , and F1 scores per class (in percentages, top scores bold).

Method	PointNet	PointNet++	Point Transformer	DGCNN
OA	71.9	75.5	78.2	82.6
μP	69.6	73.0	75.8	80.0
μR	68.1	73.0	76.6	81.8
$\mu F1$	68.1	72.6	76.1	80.4
μIoU	55.8	59.8	63.9	68.5
floor	92.3	87.6	90.7	92.1
decoration	26.2	47.1	47.0	70.0
structural	60.9	65.5	67.0	85.2
opening	28.2	27.2	36.0	66.2
other el.	71.2	71.6	78.9	88.8

pected, all the metric scores increased when testing on aggregated LoFG2 instead of high-detail LoFG3, with OA difference maximum for PointNet of 12% and the median of approximately 10% across the tested methods (Tab. 4 and Tab. 3). When analyzing LoFG2 only, we deem the *decoration* and *opening* the most challenging classes owing to their low-performance median scores of 47% and 32%, respectively. On the other hand, we observe high to medium performance for *floor*, *structural*, and *other elements* classes, that median scores were approximately 91%, 66%, 75%, respectively.

Notably networks performance ranking also varied depending on the generalization level, corroborating our assumption that methods' performance is largely depen-

dent on the segmentation objective classes: At LoFG2 the DGCNN outperformed the Point Transformer network (e.g., in recall by around 5%), and vice versa for LoFG3 (e.g., in recall by around 9%). Per-class analysis at LoFG3 also unveils that transformer-based network (PT) can have higher scores on different classes than the graph-based network (DGCNN).

6. Conclusion

In this work, we present ZAHA: a) The hierarchical segmentation classes for facade segmentation, called Level of Facade Generalization (LoFG), designed based on the international facade-related standards; b) Complemented by the classes realization on the to date largest, real-world, large-scale point cloud facade benchmark data comprising approximately 601 million points, surpassing the current largest facade benchmark four times.

The findings of this study indicate that 3D facade segmentation remains challenging and necessitates comprehensive benchmark data and unified classes introduced by LoFG. The semantic segmentation methods perform well on planar-like facade elements (up to 84% for *wall*) but struggle on intricate and sparsely represented objects (up to 5% for *deco*). We also observe that the critical elements of a facade, such as a door and a window, still necessitate novel segmentation methods (accuracy up to 22% for the door, 64% for the window). Moreover, the performance of the neural networks largely varies depending on the selected generalization level: At LoFG2 the graph-based DGCNN outperformed transformer-based Point Transformer, and inversely for LoFG3; underscoring the need for evaluation at different generalization levels.

Based on the observed trend in the 2D image-based facade segmentation domain, we firmly believe this 3D facade segmentation dataset will foster further development of 3D facade-oriented methods. Consequently, unlocking various downstream and related tasks, such as robust 3D semantic facade reconstruction for autonomous driving testing [45] or flood damage assessment [39]. We plan to extend our work by organizing a 3D facade semantic segmentation challenge and leaderboard³ to further facilitate these developments.

Acknowledgments The work was conducted within the framework of the Leonhard Obermeyer Center at the Technical University of Munich (TUM). The work on this project commenced already in 2020 and was accomplished thanks to support of various groups and researchers: The special mention goes to Jiarui Zhang, Yue Tan, Chenkun Zhang, and Prabin Gyawali, for their diligent work in the annotation process.

³Leaderboard: <https://tum2t.win/benchmarks/pc-fac>

References

- [1] Sam Amirebrahimi, Abbas Rajabifard, Priyan Mendis, and Tuan Ngo. A BIM-GIS integration method in support of the assessment and 3D visualisation of flood damage to a building. *Journal of Spatial Science*, 61(2):317–350, 2016. **1**
- [2] Julia Barbosa, Benedikt Schwab, Olaf Wysocki, Medhini Heeramaglore, and Xiaoyu Huang. tum2twin: repository of CityGML LoD3 models of the technical university of munich. <https://github.com/tum-gis/tum2twin/tree/main>, 2023. Accessed: 2023-09-22. **4**
- [3] Carlo Battini, Umberto Ferretti, Giorgia De Angelis, Roberto Pierdicca, Marina Paolanti, and Ramona Quattrini. Automatic generation of synthetic heritage point clouds: Analysis and segmentation based on shape grammar for historical vaults. *Journal of Cultural Heritage*, 66:37–47, 2024. **3**
- [4] S. Blaser, J. Meyer, and S. Nebiker. Open urban and forest datasets from a high-performance mobile mapping backpack – a contribution for advancing the creation of digital city twins. *The International Archives of the Photogrammetry, Remote Sensing and Spatial Information Sciences*, XLIII-B1-2021:125–131, 2021. **3**
- [5] B. Borgmann, V. Schatz, H. Kieritz, C. Scherer-Klößling, M. Hebel, and M. Arens. Data processing and recording using a versatile multi-sensor vehicle. *ISPRS Annals of the Photogrammetry, Remote Sensing and Spatial Information Sciences*, IV-1:21–28, 2018. **4**
- [6] Claus Brenner and Nora Ripperda. Extraction of facades using RJMCMC and constraint equations. *Photogrammetric Computer Vision*, 36:155–160, 2006. **3**
- [7] Angela Dai, Angel X Chang, Manolis Savva, Maciej Halber, Thomas Funkhouser, and Matthias Nießner. Scannet: Richly-annotated 3d reconstructions of indoor scenes. In *Proceedings of the IEEE conference on computer vision and pattern recognition*, pages 5828–5839, 2017. **3, 6**
- [8] Mark De Deuge, Alastair Quadros, Calvin Hung, and Bertrand Douillard. Unsupervised feature learning for classification of outdoor 3d scans. *Australasian Conference on Robotics and Automation*, 2(1), 2013. **3**
- [9] Jean-Emmanuel Deschaud, David Duque, Jean Pierre Richa, Santiago Velasco-Forero, Beatriz Marcotegui, and François Goulette. Paris-CARLA-3D: A real and synthetic outdoor point cloud dataset for challenging tasks in 3D mapping. *Remote Sensing*, 13(22):4713, 2021. **3**
- [10] Zhen Dong, Fuxun Liang, Bisheng Yang, Yusheng Xu, Yufu Zang, Jianping Li, Yuan Wang, Wenxia Dai, Hongchao Fan, Juha Hyypä, et al. Registration of large-scale terrestrial laser scanner point clouds: A review and benchmark. *ISPRS Journal of Photogrammetry and Remote Sensing*, 163:327–342, 2020. **3**
- [11] Johannes Flotzinger, Philipp J Rösch, Christian Benz, Muneer Ahmad, Murat Cankaya, Helmut Mayer, Volker Rodehorst, Norbert Oswald, and Thomas Braml. Dac-challenge: Semantic segmentation during visual bridge inspections. *Proceedings of the IEEE/CVF Winter Conference on Applications of Computer Vision*, pages 716–725, 2024. **3**
- [12] Raghudeep Gadde, Renaud Marlet, and Nikos Paragios. Learning grammars for architecture-specific facade parsing. *International Journal of Computer Vision*, 117(3):290–316, 2016. **2**
- [13] Jakob Geyer, Yohannes Kassahun, Mentar Mahmudi, Xavier Ricou, Rupesh Durgesh, Andrew S Chung, Lorenz Hauswald, Viet Hoang Pham, Maximilian Mühlegg, Sebastian Dorn, et al. A2D2: Audi autonomous driving dataset. *arXiv preprint arXiv:2004.06320*, 2020. **3**
- [14] Silvia María González-Collazo, Jesús Balado, Iván Garrido, Javier Grandío, Rabia Rashdi, Elisavet Tsiranidou, Pablo del Río-Barral, Erik Rúa, Iván Puente, and Henrique Lorenzo. Santiago urban dataset sud: Combination of handheld and mobile laser scanning point clouds. *Expert Systems with Applications*, 238:121842, 2024. **3**
- [15] David Griffiths and Jan Boehm. SynthCity: A large scale synthetic point cloud. *arXiv preprint arXiv:1907.04758*, 2019. **3**
- [16] Eleonora Grilli and Fabio Remondino. Machine learning generalisation across different 3D architectural heritage. *ISPRS International Journal of Geo-Information*, 9(6):379, 2020. **3, 7**
- [17] Gerhard Gröger, Thomas H Kolbe, Claus Nagel, and Karl-Heinz Häfele. OGC City Geography Markup Language CityGML Encoding Standard, 2012. Open Geospatial Consortium: Wayland, MA, USA, 2012. **1, 2, 4, 5**
- [18] Timo Hackel, Nikolay Savinov, Lubor Ladicky, Jan D Wegner, Konrad Schindler, and Marc Pollefeys. Semantic3d.net: A new large-scale point cloud classification benchmark. *arXiv preprint arXiv:1704.03847*, 2017. **3**
- [19] Simon Hensel, Steffen Goebels, and Martin Kada. Facade reconstruction for textured LOD2 CityGML models based on deep learning and mixed integer linear programming. *ISPRS Annals of the Photogrammetry, Remote Sensing and Spatial Information Sciences*, IV-2/W5:37–44, 2019. **3**
- [20] Leica Geosystems Hexagon. Cyclone 3dr, 2024.01. <https://cyclone3dr.com/downloads.php>, 2024. Accessed: 2024-01-30. **6**
- [21] Hitachi. Semantic segmentation editor. <https://github.com/Hitachi-Automotive-And-Industry-Lab/semantic-segmentation-editor>, 2021. Accessed: 2024-01-30. **6**
- [22] Hai Huang, Mario Michelini, Matthias Schmitz, Lukas Roth, and Helmut Mayer. LOD3 building reconstruction from multi-source images. *The International Archives of the Photogrammetry, Remote Sensing and Spatial Information Sciences*, XLIII-B2-2020:427–434, 2020. **3**
- [23] Anna Klimkowska, Stefano Cavazzi, Richard Leach, and Stephen Grebby. Detailed three-dimensional building façade reconstruction: A review on applications, data and technologies. *Remote Sensing*, 14(11):2579, 2022. **1**
- [24] Thomas H. Kolbe and Andreas Donaubaue. Semantic 3D city modeling and BIM. In Wenzhong Shi, Michael F. Goodchild, Michael Batty, Mei-Po Kwan, and Anshu Zhang, editors, *Urban Informatics*, pages 609–636, Singapore, 2021. Springer Singapore. **2, 3**
- [25] Thomas H Kolbe, Gerhard Gröger, and Lutz Plümer. CityGML–3D city models and their potential for emergency

- response. *Geospatial Information Technology for Emergency Response*, 257:273–290, 2008. 2
- [26] Filip Korc and Wolfgang Förstner. eTRIMS image database for interpreting images of man-made scenes. *Department of Photogrammetry, University of Bonn, Technical Report TR-IGG-P-2009-01*, pages 1–12, 2009. 1, 2
- [27] Tatjana Kutzner, Kanishk Chaturvedi, and Thomas H. Kolbe. CityGML 3.0: New functions open up new applications. *PFG – Journal of Photogrammetry, Remote Sensing and Geoinformation Science*, 88(1):1–19, 2020. 3, 4
- [28] Mikael Laakso and AO Kiviniemi. The IFC standard: A review of history, development, and standardization, information technology. *ITcon*, 17(9), 2012. 3
- [29] Monique Berger Lande. Automatic registration of partially overlapping terrestrial laser scanner point clouds. https://prs.igp.ethz.ch/research/completed_projects/automatic_registration_of_point_clouds.html, 2012. Accessed: 2020-10-30. 3
- [30] Ying Li, Lingfei Ma, Zilong Zhong, Fei Liu, Michael A Chapman, Dongpu Cao, and Jonathan Li. Deep learning for lidar point clouds in autonomous driving: A review. *IEEE Transactions on Neural Networks and Learning Systems*, 32(8):3412–3432, 2020. 1, 6
- [31] Yiyi Liao, Jun Xie, and Andreas Geiger. KITTI-360: A novel dataset and benchmarks for urban scene understanding in 2D and 3D. *arXiv preprint arXiv:2109.13410*, 2021. 3
- [32] Hantang Liu, Yinghao Xu, Jialiang Zhang, Jianke Zhu, Yang Li, and Steven CH Hoi. DeepFacade: A deep learning approach to facade parsing with symmetric loss. *IEEE Transactions on Multimedia*, 22(12):3153–3165, 2020. 1, 3
- [33] Romain Loiseau, Mathieu Aubry, and Loïc Landrieu. Online segmentation of lidar sequences: Dataset and algorithm. In Shai Avidan, Gabriel Brostow, Moustapha Cissé, Giovanni Maria Farinella, and Tal Hassner, editors, *Computer Vision – ECCV 2022*, pages 301–317, Cham, 2022. Springer Nature Switzerland. 3
- [34] Francesca Matrone, Eleonora Grilli, Massimo Martini, Marina Paolanti, Roberto Pierdicca, and Fabio Remondino. Comparing machine and deep learning methods for large 3D heritage semantic segmentation. *ISPRS International Journal of Geo-Information*, 9(9):535, 2020. 3, 4, 7
- [35] F. Matrone, A. Lingua, R. Pierdicca, E. S. Malinverni, M. Paolanti, E. Grilli, F. Remondino, A. Murtiyoso, and T. Landes. A benchmark for large-scale heritage point cloud semantic segmentation. *The International Archives of the Photogrammetry, Remote Sensing and Spatial Information Sciences*, XLIII-B2-2020:1419–1426, 2020. 1, 2, 3, 6
- [36] Helmut Mayer and Sergiy Reznik. Building facade interpretation from uncalibrated wide-baseline image sequences. *ISPRS Journal of Photogrammetry and Remote Sensing*, 61(6):371–380, 2007. 3
- [37] Daniel Munoz, J. Andrew (Drew) Bagnell, Nicolas Vandapel, and Martial Hebert. Contextual classification with functional Max-Margin Markov networks. *IEEE/CVF Conference on Computer Vision and Pattern Recognition (CVPR)*, pages 975 – 982, June 2009. 2, 3
- [38] Przemyslaw Musialski, Peter Wonka, Daniel G Aliaga, Michael Wimmer, Luc Van Gool, and Werner Purgathofer. A survey of urban reconstruction. *Computer graphics forum*, 32(6):146–177, 2013. 1, 3
- [39] Romain Nouvel, Claudia Schulte, Ursula Eicker, Dirk Pietruschka, and Volker Coors. CityGML-based 3D city model for energy diagnostics and urban energy policy support. *IBPSA World*, 2013:1–7, 2013. 8
- [40] Roberto Pierdicca, Marina Paolanti, Francesca Matrone, Massimo Martini, Christian Morbidoni, Eva Savina Malinverni, Emanuele Frontoni, and Andrea Maria Lingua. Point cloud semantic segmentation using a deep learning framework for cultural heritage. *Remote Sensing*, 12(6):1005, 2020. 3, 6, 7
- [41] Charles R Qi, Hao Su, Kaichun Mo, and Leonidas J Guibas. PointNet: Deep learning on point sets for 3d classification and segmentation. *IEEE/CVF Conference on Computer Vision and Pattern Recognition (CVPR)*, pages 652–660, 2017. 3, 7
- [42] Charles Ruizhongtai Qi, Li Yi, Hao Su, and Leonidas J Guibas. PointNet++: Deep hierarchical feature learning on point sets in a metric space. *Advances in Neural Information Processing System (NeurIPS)*, 30, 2017. 3, 7
- [43] Hayko Riemenschneider, Ulrich Krispel, Wolfgang Thaller, Michael Donoser, Sven Havemann, Dieter Fellner, and Horst Bischof. Irregular lattices for complex shape grammar facade parsing. *IEEE/CVF Conference on Computer Vision and Pattern Recognition (CVPR)*, pages 1640–1647, 2012. 2
- [44] Xavier Roynard, Jean-Emmanuel Deschaud, and François Goulette. Paris-Lille-3D: A large and high-quality ground-truth urban point cloud dataset for automatic segmentation and classification. *The International Journal of Robotics Research*, 37(6):545–557, 2018. 3
- [45] Benedikt Schwab and Thomas H Kolbe. Requirement analysis of 3D road space models for automated driving. *ISPRS Annals of the Photogrammetry, Remote Sensing and Spatial Information Sciences*, IV-4/W8:99–106, 2019. 1, 8
- [46] Sophia Schwarz, Tanja Pilz, Olaf Wysocki, Ludwig Hoegner, and Uwe Stilla. Transferring facade labels between point clouds with semantic octrees while considering change detection. *International 3D GeoInfo Conference 2023, Recent Advances in 3D Geoinformation Science*, pages 287–298, 2023. 4
- [47] Andrés Serna, Beatriz Marcotegui, François Goulette, and Jean-Emmanuel Deschaud. Paris-rue-Madame database: As 3D mobile laser scanner dataset for benchmarking urban detection, segmentation and classification methods. In *Proceedings of the International Conference on Pattern Recognition Applications and Methods. ACM, Angers, France, 6–8 March*, pages 819–824, 2014. 2, 3
- [48] Shuo Shen, Yan Xia, Andreas Eich, Yusheng Xu, Bisheng Yang, and Uwe Stilla. Segtrans: Semantic segmentation with transfer learning for mls point clouds. *IEEE Geoscience and Remote Sensing Letters*, 2023. 4
- [49] Special Interest Group 3D. Modeling Guide for 3D Objects - Part 2: Modeling of Buildings (LoD1, LoD2, LoD3) - codelist English. *SIG3D Quality Working Group*, 2020. Accessed: 2023-01-30. 5

- [50] Special Interest Group 3D. Modeling Guide for 3D Objects - Part 2: Modeling of Buildings (LoD1, LoD2, LoD3) - codelist German. *SIG3D Quality Working Group*, 2020. Accessed: 2023-01-30. [5](#)
- [51] Richard Szeliski. *Computer vision: Algorithms and applications*. Springer Science & Business Media, 2010. [1](#), [2](#), [3](#)
- [52] Weikai Tan, Nannan Qin, Lingfei Ma, Ying Li, Jing Du, Guorong Cai, Ke Yang, and Jonathan Li. Toronto-3D: A large-scale mobile LiDAR dataset for semantic segmentation of urban roadways. In *IEEE/CVF Conference on Computer Vision and Pattern Recognition Workshops (CVPRW)*, pages 202–203, 2020. [1](#), [3](#), [7](#)
- [53] Yue Tan, Olaf Wysocki, Ludwig Hoegner, and Uwe Stilla. Classifying point clouds at the facade-level using geometric features and deep learning networks. *International 3D GeoInfo Conference 2023, Recent Advances in 3D Geoinformation Science*, pages 391–404, 2023. [3](#)
- [54] Hugues Thomas, Charles R Qi, Jean-Emmanuel Deschaud, Beatriz Marcotegui, François Goulette, and Leonidas J Guibas. Kpconv: Flexible and deformable convolution for point clouds. *IEEE/CVF International Conference on Computer Vision (ICCV)*, pages 6411–6420, 2019. [3](#)
- [55] Sebastian Tuttas and Uwe Stilla. Reconstruction of façades in point clouds from multi aspect oblique ALS. *ISPRS Annals of the Photogrammetry, Remote Sensing and Spatial Information Sciences*, II-3/W3:91–96, 2013. [4](#)
- [56] Radim Tyleček and Radim Šára. Spatial pattern templates for recognition of objects with regular structure. In *German Conference on Pattern Recognition, Saarbrücken, Germany, September 3-6, 2013*, pages 364–374. Springer, 2013. [2](#)
- [57] Bruno Vallet, Mathieu Brédif, Andrés Serna, Beatriz Marcotegui, and Nicolas Paparoditis. TerraMobilita/iQmulus urban point cloud analysis benchmark. *Computers & Graphics*, 49:126–133, 2015. [3](#)
- [58] Bayerische Vermessungsverwaltung. 3D-Gebäudemodelle (LoD2). <https://geodaten.bayern.de/opengeodata/OpenDataDetail.html?pn=lod2>, 2023. Accessed: 2023-01-30. [4](#)
- [59] Ruisheng Wang, Shangfeng Huang, and Hongxin Yang. Building3d: A urban-scale dataset and benchmarks for learning roof structures from point clouds. In *Proceedings of the IEEE/CVF International Conference on Computer Vision*, pages 20076–20086, 2023. [7](#)
- [60] Yue Wang, Yongbin Sun, Ziwei Liu, Sanjay E Sarma, Michael M Bronstein, and Justin M Solomon. Dynamic graph cnn for learning on point clouds. *ACM Transactions on Graphics (tog)*, 38(5):1–12, 2019. [3](#), [7](#)
- [61] Bruno Willenborg, Martin Pültz, and Thomas H Kolbe. Integration of semantic 3D city models and 3D mesh models for accuracy improvements of solar potential analyses. *The International Archives of the Photogrammetry, Remote Sensing and Spatial Information Sciences*, XLII-4/W10:223–230, 2018. [1](#)
- [62] Olaf Wysocki, Eleonora Grilli, Ludwig Hoegner, and Uwe Stilla. Combining visibility analysis and deep learning for refinement of semantic 3D building models by conflict classification. *ISPRS Annals of the Photogrammetry, Remote Sensing and Spatial Information Sciences*, X-4/W2-2022:289–296, 2022. [3](#), [6](#)
- [63] Olaf Wysocki, Ludwig Hoegner, and Uwe Stilla. TUM-FAÇADE: Reviewing and enriching point cloud benchmarks for façade segmentation. *The International Archives of the Photogrammetry, Remote Sensing and Spatial Information Sciences*, XLVI-2/W1-2022:529–536, 2022. [1](#), [2](#), [3](#), [4](#), [6](#)
- [64] Olaf Wysocki, Ludwig Hoegner, and Uwe Stilla. MLS2LoD3: Refining low lods building models with mls point clouds to reconstruct semantic lod3 building models. *International 3D GeoInfo Conference 2023, Recent Advances in 3D Geoinformation Science*, pages 367–380, 2023. [1](#)
- [65] Olaf Wysocki, Benedikt Schwab, Christof Beil, Christoph Holst, and Thomas H Kolbe. Reviewing open data semantic 3D city models to develop novel 3D reconstruction methods. *The International Archives of the Photogrammetry, Remote Sensing and Spatial Information Sciences*, 48:493–500, 2024. [2](#)
- [66] Olaf Wysocki, Yan Xia, Magdalena Wysocki, Eleonora Grilli, Ludwig Hoegner, Daniel Cremers, and Uwe Stilla. Scan2LoD3: Reconstructing semantic 3D building models at LoD3 using ray casting and Bayesian networks. *IEEE/CVF Conference on Computer Vision and Pattern Recognition Workshops (CVPRW)*, pages 6547–6557, 2023. [1](#), [3](#), [4](#)
- [67] Yan Xia, Yusheng Xu, Cheng Wang, and Uwe Stilla. VPC-Net: Completion of 3D vehicles from MLS point clouds. *ISPRS Journal of Photogrammetry and Remote Sensing*, 174:166–181, 2021. [3](#)
- [68] Yusheng Xu and Uwe Stilla. Towards building and civil infrastructure reconstruction from point clouds: A review on data and key techniques. *IEEE Journal of Selected Topics in Applied Earth Observations and Remote Sensing*, 14:2857–2885, 2021. [1](#), [3](#)
- [69] Chandan Yeshwanth, Yueh-Cheng Liu, Matthias Nießner, and Angela Dai. ScanNet++: A high-fidelity dataset of 3d indoor scenes. In *Proceedings of the IEEE/CVF International Conference on Computer Vision*, pages 12–22, 2023. [3](#), [6](#)
- [70] Yifan Zhang, Bingyi Kang, Bryan Hooi, Shuicheng Yan, and Jiashi Feng. Deep long-tailed learning: A survey. *IEEE Transactions on Pattern Analysis and Machine Intelligence*, 2023. [3](#), [6](#)
- [71] Hengshuang Zhao, Li Jiang, Jiaya Jia, Philip HS Torr, and Vladlen Koltun. Point transformer. *IEEE/CVF International Conference on Computer Vision (ICCV)*, pages 16259–16268, 2021. [3](#), [7](#)
- [72] Jingwei Zhu, Joachim Gehring, Rong Huang, Björn Borgmann, Zhenghao Sun, Ludwig Hoegner, Marcus Hebel, Yusheng Xu, and Uwe Stilla. TUM-MLS-2016: An annotated mobile LiDAR dataset of the TUM City Campus for semantic point cloud interpretation in urban areas. *Remote Sensing*, 12(11):1875, 2020. [3](#), [4](#)

The supplementary material to: "ZAHA: Introducing the Level of Facade Generalization and the Large-Scale Point Cloud Facade Semantic Segmentation Benchmark Dataset"

A. Experiments

A.1. Evaluation Metrics

To evaluate the performance of the 3D facade segmentation, we used the established semantic segmentation network metrics, such as Overall Accuracy, Precision, Recall, and Jaccard Index also known as Intersection over Union (IoU) [2]. They were defined as follows:

$$\text{Overall Accuracy} = \frac{\text{True Positives} + \text{True Negatives}}{\text{Total Instances}}$$

$$\text{Precision} = \frac{\text{True Positives}}{\text{True Positives} + \text{False Positives}}$$

$$\text{Recall} = \frac{\text{True Positives}}{\text{True Positives} + \text{False Negatives}}$$

$$F1 = 2 \times \frac{\text{Precision} \times \text{Recall}}{\text{Precision} + \text{Recall}}$$

$$\begin{aligned} \text{IoU} &= \frac{\text{Intersection Area}}{\text{Union Area}} = \\ &= \frac{\text{True Positives}}{\text{True Positives} + \text{False Positives} + \text{False Negatives}} \end{aligned}$$

A.2. Parameter Settings

We conducted all the experiments using an NVIDIA GeForce RTX 4090 GPU with 16 GB VRAM with a fixed number of 100 epochs per training. The implementation will be released under our repository web page.¹

To train the PointNet and PointNet++, we utilized the implementation sourced from [3, 4, 9]. We used the point cloud coordinates as input layers to adapt the model and modify the corresponding classes. We employed a batch size of 32 for training and testing, and each batch contains 1024 points per sample point cloud. Stochastic gradient descent with a momentum of 0.1 and a learning rate 0.001 was employed.

To train the Point Transformer, we used the implementation of the first author of Point Transformer [11], in [10]. Diverging from the voxelization method employed in the source code to generate batches, we have opted for a batch design strategy based on index segmentation. Consistent with previous experiments, we also utilized a batch size of 32 as input and 1024 points per sample point cloud. Stochastic gradient descent with a momentum of 0.9 and an initial learning rate of 0.1 was employed. After 60 epochs, the learning rate would reduced to 0.01, and after 80 epochs, 0.001.

To train the DGCNN, we utilized the implementation sourced from [5, 8]. We customized their implementation by adjusting the dimensions of the input and output layers to suit the dimensionality and the number of classes. During training, we employed a batch size of 32, while for testing, we used a batch size of 16, each containing 1024 points per sample point cloud. Stochastic gradient descent with a momentum of 0.9 and a learning rate of 0.1 was employed. We set the dropout rate to 0.5 and the number of nearest neighbors that we considered to 20.

A.3. Extra Baseline Experiment on a Large-Scale-Oriented Network

Owing to the space limitation and similar performance scores to the other networks, we have moved the extra experiments on the large-scale-oriented KPConv [6] network to the supplemental material. Here, we show the extra set of experiments that we conducted on the KPConv network, whereby we also fine-tuned the hyper-parameters. KPConv introduces a deformable convolution operation, allowing the neural network to learn flexible and adaptive convolutional filters. The use of kernel points in KPConv allows for more efficient processing of point clouds, and as such, it has often been used in the context of large-scale, outdoor point clouds [1]. However, corroborating our experiment results in the main paper, there were no significant performance differences observed, as we visualize in Figure 1 and Figure 2, and list in Table 1 and Table 2.

To train the KPConv, we employed the implementation sourced from [6, 7]. The input radius of the input sphere was

¹Project page: <https://github.com/OloOcki/zaha>

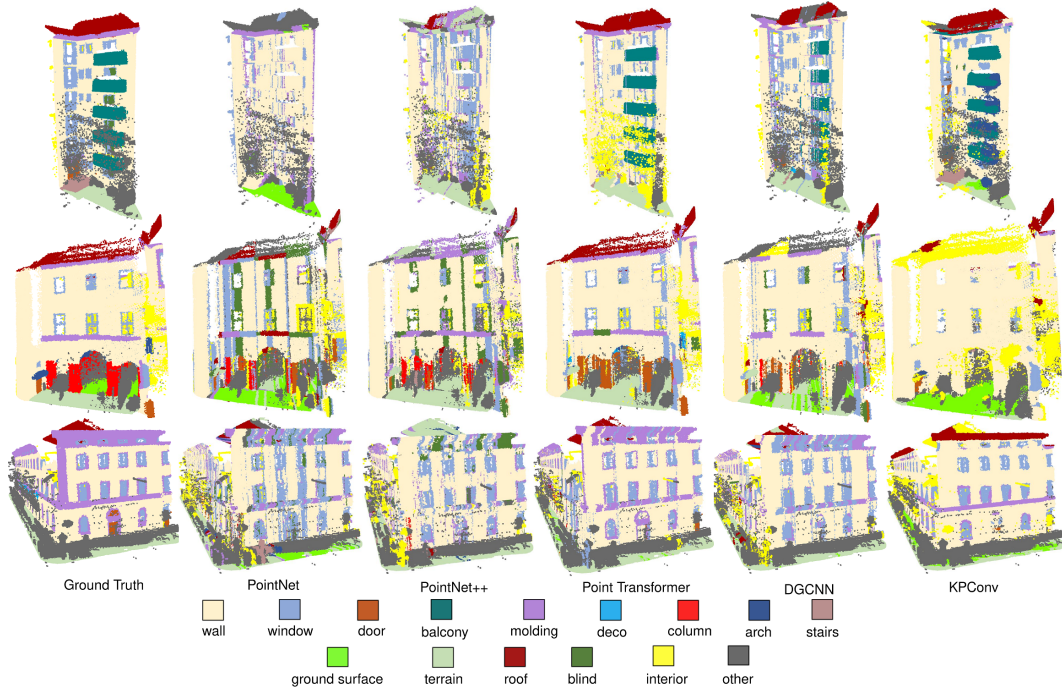


Figure 1. LoFG3 inference on the test set comprising residential (top), underpass and cultural heritage (middle), and university buildings (bottom) with the extra fine-tuned KPConv.

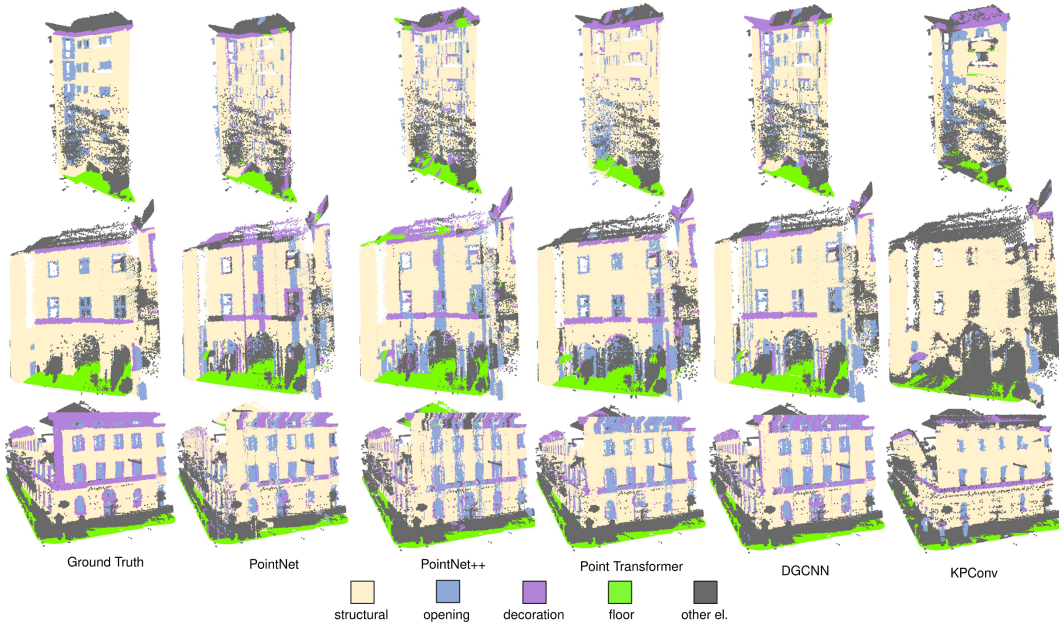


Figure 2. LoFG2 inference on the test set comprising residential (top), underpass and cultural heritage (middle), and university buildings (bottom); color-coding according to the most prominent merged sub-class with the extra fine-tuned KPConv.

set as 1.5m. We also generated the radius of deformable convolution in the "number grid cell" as 1.5m, to minimize noisy clusters. For both baselines, we set the epoch steps as 2000 and the validation size as 100. The batch size was set

to 6 for training and 1 for testing. For the training of LoFG2, stochastic gradient descent with a momentum of 0.98 and a learning rate of 0.001 was employed, and there were 150 training epochs. For the training of LoFG3, stochastic gra-

Table 1. LoFG3 test: OA, μP , μR , $\mu F1$, μIoU , and F1 scores per class, in percentages; with the extra fine-tuned KPConv

Method	PointNet	PointNet++	Point Transformer	DGCNN	KPConv
OA	59.9	66.4	75.0	71.1	65.2
μP	46.1	37.8	52.7	53.6	46.4
μR	42.2	35.9	54.7	45.8	44.6
$\mu F1$	38.7	34.8	52.1	44.5	39.3
μIoU	26.4	25.6	41.6	33.4	28.6
wall	61.1	68.5	76.8	83.8	66.6
window	25.6	26.3	43.1	64.1	41.0
door	13.5	7.8	19.8	21.6	9.6
balcony	25.1	0.0	77.5	66.7	61.7
molding	22.5	43.4	58.0	57.5	23.3
deco	0.0	0.0	5.0	0.0	0.0
column	22.4	33.4	0.0	37.2	0.0
arch	19.2	25.4	50.2	2.6	11.5
stairs	16.0	0.0	7.5	5.6	6.5
ground surface	12.0	0.0	24.4	21.3	26.3
terrain	53.5	53.5	57.6	68.0	31.4
roof	18.7	6.8	66.3	57.4	15.4
blinds	4.6	2.3	18.5	20.0	10.0
interior	59.7	69.1	72.8	88.0	75.1
other	42.7	47.1	70.6	74.1	50.0

Table 2. LoFG2 test: OA, μP , μR , $\mu F1$, μIoU , and F1 scores per class, in percentages; with the extra fine-tuned KPConv

Method	PointNet	PointNet++	Point Transformer	DGCNN	KPConv
OA	71.9	75.5	78.2	82.6	71.6
μP	69.6	73.0	75.8	80.0	71.2
μR	68.1	73.0	76.6	81.8	64.3
$\mu F1$	68.1	72.6	76.1	80.4	66.4
μIoU	55.8	59.8	63.9	68.5	52.3
floor	92.3	87.6	90.7	92.1	80.1
decoration	26.2	47.1	47.0	70.0	28.2
structural	60.9	65.5	67.0	85.2	62.4
opening	28.2	27.2	36.0	66.2	31.7
other el.	71.2	71.6	78.9	88.8	58.5

dient descent with a momentum of 0.98 and a learning rate of 0.01 was employed, and the training epochs were set as the default number 500.

A.4. Benchmark and Leaderboard

We introduce the ZAHA as a benchmark to foster the research on facade semantic segmentation. It is a common practice to publish a leaderboard, which encourages researchers to delve into a challenge. We initialize the leaderboard at the webpage² and invite researchers to develop novel and more efficient facade segmentation methods.

A.5. Extra visuals

Additional visuals are included at the project page³ showing an animated gif file, and the full dataset and annotations according to the 15 introduced classes at LoFG3 and their generalization at LoFG2.

References

- [1] Martin Kada and Dmitry Kuramin. Als point cloud classification using pointnet++ and kpconv with prior knowledge.

²Leaderboard: <https://tum2t.win/benchmarks/pc-fac>

³Project page: <https://github.com/OloOcki/zaha>

The International Archives of the Photogrammetry, Remote Sensing and Spatial Information Sciences, 46:91–96, 2021.

- [2] Ying Li, Lingfei Ma, Zilong Zhong, Fei Liu, Michael A Chapman, Dongpu Cao, and Jonathan Li. Deep learning for lidar point clouds in autonomous driving: A review. *IEEE Transactions on Neural Networks and Learning Systems*, 32(8):3412–3432, 2020. 1
- [3] Charles R Qi, Hao Su, Kaichun Mo, and Leonidas J Guibas. PointNet: Deep learning on point sets for 3d classification and segmentation. *IEEE/CVF Conference on Computer Vision and Pattern Recognition (CVPR)*, pages 652–660, 2017. 1
- [4] Charles Ruizhongtai Qi, Li Yi, Hao Su, and Leonidas J Guibas. PointNet++: Deep hierarchical feature learning on point sets in a metric space. *Advances in Neural Information Processing System (NeurIPS)*, 30, 2017. 1
- [5] An Tao. dgcn.pytorch. <https://github.com/antao97/dgcnn.pytorch>, 2024. Accessed: 2024-03-06. 1
- [6] Hugues Thomas, Charles R Qi, Jean-Emmanuel Deschaud, Beatriz Marcotegui, François Goulette, and Leonidas J Guibas. Kpconv: Flexible and deformable convolution for point clouds. *IEEE/CVF International Conference on Computer Vision (ICCV)*, pages 6411–6420, 2019. 1
- [7] Hugues Thomas, Charles R. Qi, Jean-Emmanuel Deschaud, Beatriz Marcotegui, François Goulette, and Leonidas J. Guibas. KPConv pytorch. <https://github.com/HuguesTHOMAS/KPConv-PyTorch>, 2019. Accessed: 2024-03-06. 1
- [8] Yue Wang, Yongbin Sun, Ziwei Liu, Sanjay E Sarma, Michael M Bronstein, and Justin M Solomon. Dynamic graph cnn for learning on point clouds. *ACM Transactions on Graphics (tog)*, 38(5):1–12, 2019. 1
- [9] Xu Yan. Pointnet/pointnet++ pytorch. https://github.com/yanx27/Pointnet_Pointnet2_pytorch, 2019. Accessed: 2024-03-06. 1
- [10] Hengshuang Zhao. point-transformer. <https://github.com/POSTECH-CVLab/point-transformer>, 2021. Accessed: 2024-03-06. 1
- [11] Hengshuang Zhao, Li Jiang, Jiaya Jia, Philip HS Torr, and Vladlen Koltun. Point transformer. *IEEE/CVF International Conference on Computer Vision (ICCV)*, pages 16259–16268, 2021. 1